Stellar Population Models

Claudia Maraston

Max-Planck-Institut für extraterrestrische Physik, Garching, Germany

Abstract. This review deals with stellar population models computed by means of the *evolutionary synthesis* technique that was pioneered by Beatrice Tinsley roughly three decades ago. The focus is on the simplest models, the so called *Simple Stellar Populations*, that describe instantaneous generations of single stars with the same chemical composition and age. The development of these models until very recent results is discussed, pinpointing the model uncertainties that have been solved and those that still demand a cautionary use of the models. The fundamental step of calibrating the models with *galactic* globular clusters, for which ages and element abundances are known independently, is illustrated by means of key examples.

1 Introduction

The evolutionary population synthesis (EPS) is the technique to model the spectrophotometric properties of stellar populations, that uses the knowledge of stellar evolution. This approach was pioneered by B. Tinsley (see Section 3.1) in a series of fundamental papers, that provide the basic concepts still used in present-day models. The target of EPS models are those stellar systems that cannot be resolved into single stars, like galaxies and extra-galactic globular clusters. The comparison with the models aims at providing clues on the ages and element abundances of these unresolved stellar populations, in order to constrain their formation processes, and finds ubiquitous astrophysical uses. The simplest flavour of an EPS model, called *Simple Stellar Population* (hereafter SSP), assumes that all stars are coeval and share the same chemical composition. The advantage of dealing with SSPs is twofold. First, SSPs can be compared directly with globular cluster (hereafter GC) data, since these are the "simplest" stellar populations in nature. This offers the advantage of *calibrating* the SSPs with those GCs for which ages and element abundances are independently known ([35]). This step is crucial to fix the parameters that are used to describe that part of the model "input physics" that cannot be derived from first principle (convection, mass loss, mixing). The calibrated models can be applied with more confidence to the study of extragalactic stellar population. Second, complex stellar systems which are made up by various stellar generations are modelled by convolving SSPs with the adopted star formation history (e.g. [1], [36], [47], [19], [2]), therefore the deep knowledge of the building blocks of complex models is very important.

The article starts with a description of stellar population models in terms of ingredients, assumptions and computational technique (Section 2), which is followed by a historical overview of the evolution of these models until the most recent results (Section 3).

2 Model Structure

2.1 Ingredients

The basic ingredients of a stellar population model are the stellar evolutionary tracks and the stellar model atmospheres. The former trace the evolution of stars

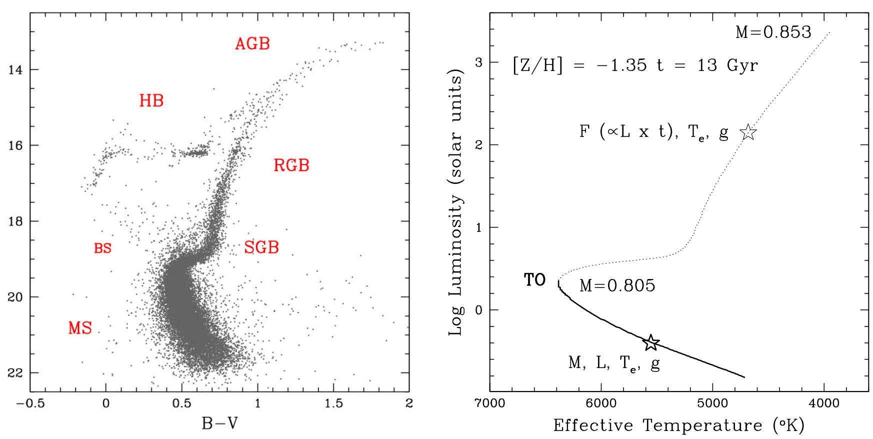

Fig. 1. *Left-hand panel* Observed color magnitude diagram (CMD) of the old, metal-poor galactic GC NGC 1851 (data from [29]). Evolutionary phases are labelled, i.e. Main Sequence (MS); Sub Giant Branch (SGB); Red Giant Branch (RGB); Horizontal Branch (HB); Asymptotic Giant Branch (AGB). BS mean blue stragglers. *Right-hand panel.* Theoretical H-R diagram of an old, metal-poor SSP, up to the RGB-tip (isochrone from [10]). Solid and dotted linestyles mark Main Sequence and post Main Sequence, respectively. Stellar masses at the turnoff (TO) and RGB-tip are given.

of given mass and chemical composition through the various evolutionary phases (Figure 1), providing the basic stellar parameters - bolometric luminosities L; effective temperatures $T_{\rm eff}$; surface gravities g - as functions of evolutionary timescales. The model atmospheres describe the emergent flux as a function of these parameters, which allows the computation of the stellar spectral energy distribution (SED).

Various sets of stellar tracks exist in the literature, which can be divided into two main groups according to whether the *convective overshooting* is accounted for or not. Examples of overshooting tracks are the Padova (e.g. [15]), the Geneva ([24]) and the Yale tracks (see Yi, this volume). Stellar tracks which do not include overshooting are those by e.g. [45] and [10]. The actual size of overshooting is still a matter of debate among the various groups, but recent works favour

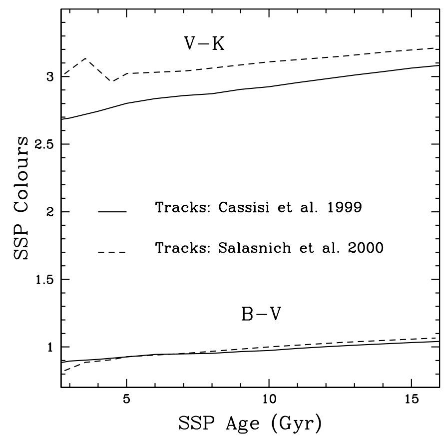

Fig. 2. Impact of the temperature of the RGB as described by different tracks, on SSP colors.

small values (see Yi, this volume). The temperature of the Red Giant Branch is the most discrepant quantity among the stellar tracks, that results in the largest differences among the SSP output. This is shown in Figure 2 that compares the B−V and V−K colors of SSP models with solar metallicity and various ages computed with two different sets of stellar tracks, and the same EPS. While the B−V colors are virtually identical, indicating a consistent modeling of the MS, the V−K colours that depend strongly on the RGB, are very different. A measured V−K$\sim$ 3 is consistent with ages of $\sim$ 5 Gyr or $\sim$ 13 Gyr if the tracks by [37] or by [10] are used, respectively. This agrees with the results by [12], that attribute the large discrepancies in the V−K of their respective models almost entirely to differences in the stellar evolution prescriptions. The temperature of the RGB is determined by the mixing-length parameter, which regulates the stellar radius, hence effective temperatures. In both sets of stellar tracks the mixing-length is calibrated with the solar standard model. The reason of such a discrepancy deserves further investigation.

The most complete grid of model atmospheres is that by [20] (and revisions), which covers $T_{\rm eff} > 3500\ K$ for a wide range of metallicities and gravities, the atmospheres for cooler stars being provided by other groups (e.g. [3]). EPS modellers were forced to make a collage between the various libraries, which could introduce discrepancies in the model results. A recent improvement is due to the works of the Basel group (e.g. [22], [48]), that linked the various available libraries with the Kurucz's one, and compared the derived temperature-color relations with empirical ones, when available. The resulting library covers virtually the whole parameter space ($T_{\rm eff}$; g; [Fe/H]) required by theoretical stellar tracks, with the exception of AGB M-type and Carbon stars (see Section 3.6). The spectral resolution of the model atmospheres range between 10 and 20 Å .

2.2 Assumptions

Model assumptions are: 1) The stellar initial mass function (IMF), that provides the mass spectrum of the population. It is common to express IMFs as declining power-laws with single or multiple slopes, as it follows from empirical stellar counts. 2) The helium enrichment law $\Delta Y/\Delta Z$. 3) The amount of stellar mass-loss. Mass-loss is a very critical assumption that impacts on the typical observables of stellar populations, like colours and luminosities. Mass-loss occurs in massive stars already on the Main Sequence. In intermediate mass stars ($2 < M/M_{\odot} < 5$) it is most efficient at the Asymptotic Giant Branch (AGB) and determines the fuel and extension of the Thermally Pulsing AGB phase (herefater TP-AGB). In low-mass stars mass loss acts already along the Red Giant Branch (RGB) and determines the morphology of the subsequent Horizontal Branch (HB) phase. Since the amount of mass loss cannot be *predicted* by stellar evolution it must be *calibrated* with globular clusters data.

2.3 Computational procedures

The integrated properties of SSP models, e.g. the SED, broad-band luminosities, magnitudes and colors, are obtained from the integration of the contributions by individual stars. Two methods in the literature can be distinguished by the choice of the integration variable for the stars in the post Main Sequence phase: isochrone synthesis and fuel consumption-based methods. The right-hand panel of Figure 1 shows in the theoretical H-R diagram the isochrone of a 13 Gyr old metal-poor SSP up to the RGB-tip. The Main Sequence is populated by stars spanning a large mass range, from $\sim 0.1\ M_{\odot}$ to the turnoff mass. The stellar luminosities are proportional to a high power of the stellar masses, therefore the integrated luminosity of the Main Sequence is obtained with an integration by mass of the stellar luminosities, convolved with the IMF. In post Main Sequence phases the mass range spanned by living stars is very small (cf. labels in Figure 1), and the luminosity is no longer related primarily to the mass. For the post Main Sequence two choices are possible. 1) The evolutionary lifetime of one single mass is adopted as integration variable. In this case the synthesis is based on the *fuel consumption theorem* (see Section 3.3). 2) The integration by mass is also performed in post-Main Sequence, in which case the technique is called *isochrone synthesis* (see Section 3.4). Pros and cons of the two methods have been longely discussed in the literature (see e.g. [11], [34]). A recent viewpoint will be given elsewhere.

3 Historical overview

The past three decades have witnessed great progress in the modelling of stellar populations. In the next paragraphs I will describe the basic steps that have featured the development of these models to present-day releases, by grouping the literature works into decades. The outstanding developments in each decade are emphasized.

3.1 The 60's: the first color/time evolution

A first example of stellar population model is that of [14]. The authors describe the evolution of the B−V colour of the old open cluster M67. This is accomplished with a rudimental isochrone obtained by best fitting the observed B−V vs. $M_{\rm V}$ diagram, then aged and rejuvenated by 5 Gyr, by applying homology arguments and keeping fixed the RGB tip in the isochrones (cf. their Fig 1). Although stellar evolutionary computations have shown later that isochrones are not homologous, yet the paper is important because it recognizes that the integrated colours of stellar populations because of their sensitivity to age, can be used to date extragalactic systems.

Following the developments of the first wide sets of evolutionary tracks, [41] compute the first "galaxy" model. The evolution of colour indices from U to L is provided, using the empirical $T_{\rm eff}$-colour relations by [21]. Stellar tracks describe only the upper MS and SGB, the RGB is added empirically as well as the lower Main Sequence. The basic learnings are: i) stars must be set in numbers $\propto$ lifetimes; ii) the post-main sequence evolution is so fast that mass dispersion is not important (see Section 3.3).

3.2 The 70's: the Tinsley legacy

The 70's see the full development of B. Tinsley's fundamental work. In a series of papers (e.g. [42], [43]) the evolutionary population synthesis as a method to compute the spectrophotometric properties of galaxies is defined. Analytical approximations are provided for the main parameters., e.g. star formation rates, IMFs, chemical evolution, that are still used in nowadays models. The Tinsley's models are targeted to galaxies, and a wider discussion on them goes beyond the aim of this review. Relevant to our context is the early modeling of near infrared colours ([44]), that made evident the problem of the accuracy of the integration along the RGB. By citing the authors *".. very slight departures from equal spacing in the stellar lifetimes lead to unacceptable irregularities in color because of short-lived but energetically important points"*.

3.3 The 80's: the fuel consumption theorem

The culmination of the efforts of the 70's is the last work of B. Tinsley ([18]). The authors adopted the first release of the Yale isochrones, to which empirical RGB, AGB and lower-MS were added. The application of these models to ellipticals suggested rather young ages, of the order of a few Gyrs. Indeed, it turned out (see Figure 1 in [33]) that those Yale isochrones had an *uncalibrated* mixing-length and were found not to be able to reproduce the MS of galactic GCs. The danger at deriving ages and metallicities of unresolved stellar populations with models based on uncalibrated stellar ingredients motivated [33] to re-discuss the concept of stellar population model. First, simple models should be preferred against the more complicated realizations, for these models can be straighforwardly compared to globular clusters. By *simple* it is meant that all stars are coeval and chemically homogeneous, that is the definition of SSP à la [31]. Second, two conditions should be fulfilled: i) The use of isochrones with *calibrated* mixing-length. ii) The account of *every* evolutionary phase with its *proper* energetic contribution. Indeed in the models of the '70's major evolutionary phases (e.g. HB, AGB, Post-AGB) were not included or their contribution not properly evaluated. The *fuel consumption theorem* was used to show how much they can contribute. It defines the energy conservation law for the stellar case, and is stated as: *The contribution by any Post Main Sequence evolutionary phase to the total luminosity of a simple stellar population is proportional to the amount of nuclear fuel burned in that phase* ([31]). The bolometric budget of a

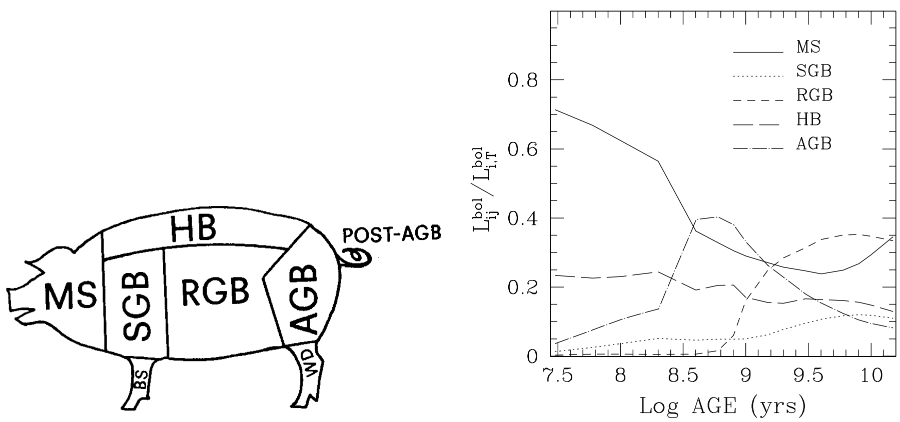

Fig. 3. An art view of the bolometric budget of a stellar population (left; from [33]) and its quantitative evaluation (right; from [25]). Evolutionary phases are labelled as in Figure 1.

SSP as a function of age, computed with the fuel consumption theorem is shown in Figure 3. The bolometric modeling of [32] is extended to the monochromatic by [7]. These models span a wide metallicity range, consider all stellar evolutionary phases and take into account various morphologies of the Horizontal Branch. However these models are computed only for old ages. [25] extends the fuel consumption approach to a wider age range (Section 3.6).

Worth noting in the same decade are the first stellar population models aimed at describing the redshift evolution of galaxies ([5]).

3.4 The 90's: isochrone synthesis

The technique called *isochrone synthesis* is by far the most popular method to compute EPS models, due to its straightforwardness of definition (see Section 2.3). The isochrone synthesis boosted with the works of Bruzual & Charlot (but see also [13]). Early implementations of the method by [5] suffered from erratic color jumps due to poor interpolation algorythms, which were later refined

([11] and [6]). Also different from the past is the use of a nearly homogeneous set of stellar ingredients, and the semi-empirical inclusion of the TP-AGB phase (see Section 3.6). Although only for solar metallicity, these models span a wide age range including for the first time very young ($t < 1$ Gyr) ages. A wider metallicity range has been provided by successive releases. These works have defined a standard technique for most models in the literature, which are constructed by applying isochrone synthesis to the isochrones released by the Geneva or by the Padova group (e.g. [38], [23], latest Worthey models, latest Vazdekis models).

3.5 The 90's: the Lick indices

Parallel to the diffusion of the isochrone synthesis, the 90's see the full development of the so-called *comprehensive* models, the feature of which is to provide the largest number of model output, e.g. broad-band colours, spectral energy distributions, mass-to-light ratios, spectral indices, surface brightness fluctuations, for the largest number of model parameters (metallicities, ages, IMFs, etc.). The most complete of these models for the study of *old* stellar populations are the models by [49]. With these a modern quantification of the age/metallicity degeneracy (e.g. [16]) has been made, which is known as the "3/2 rule" $\Delta \log \mathrm{t} / \Delta \log \mathrm{Z} \sim 3/2$. But perhaps the most important feature of the Worthey's models is to provide as first the SSP values of the whole set of the absorption line indices in the Lick system, the so-called Lick indices (Mg_2, Fe5270, Hβ, etc.). These are obtained by inserting in the Worthey's EPS code the *fitting functions* ([50]), that provide the stellar index as a function of T_{eff}, gravity and metallicity, and are constructed with real stars. Similar fitting functions for the indices Mg_2, Fe5270, Fe5335 and Hβ are provided by [8] and [9], with the corresponding SSP models in the framework of the evolutionary synthesis of [7]. When coupled with the same evolutionary synthesis these two sets of fitting functions produce consistent SSP indices ([28]). Both fitting functions by Buzzoni and Worthey do not take element abundance ratios into account but depend only on total metallicity. However, the specific abundances of given elements likely affect the absorption features, and it is known that, e.g. the magnesium-to-iron abundance ratio in Milky Way stars varies as a function of total metallicity. A step forward was made by [4], whose fitting function for Mg_2 contains the explicit dependence of the Mg abundance relative to Fe. However this approach has not been extended to other indices. Only very recently SSP models of all Lick indices in which the abundances of the specific elements are a model parameter, have been made available ([39]; see Section 3.6).

3.6 Around the turn of the century

Back to the fuel for TP-AGB The TP-AGB is perhaps the most critical stellar phase to be accounted for in a SSP model, because its energetic and extension are affected by mass-loss and nuclear burning in the envelope, both phenomena requiring parametrizations to be calibrated with data. However, the TP-AGB phase is the most important phase in intermediate-age ($0.2\ \mathrm{Gyr} \lesssim t \lesssim 1\ \mathrm{Gyr}$) stellar populations, contributing $\sim 40\%$ to the bolometric light ([32]). The fuel consumption approach allows one to include the TP-AGB phase in a SSP model in a semi-empirical way. This is done in SSP models in which the TP-AGB phase

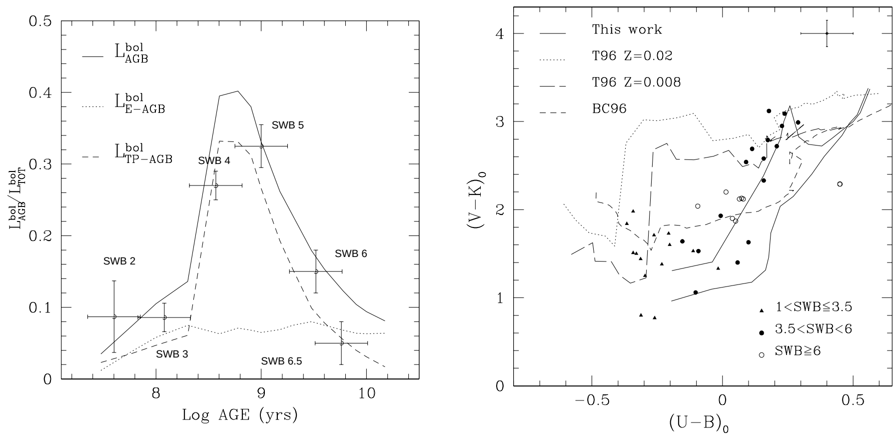

Fig. 4. *Left-hand panel.* Calibration of the bolometric contribution of the TP-AGB phase for SSP models as a function of the SSP age, with Magellanic Clouds GCs data. *Right-hand panel.* Calibration of the SSP broad-band colours V−K vs. U−B (solid thick line) with the same data. The filled circles are intermediate-age GCs. The solid thin line shows the same SSPs but without the TP-AGB phase. The other line styles show SSPs from other authors. From [25].

is calibrated with data of intermediate-age Magellanic Clouds GCs ([25]). It is shown there (and in Figure 4) that the inclusion of this phase is crucial to match the integrated near-IR colours of these clusters. The calibrated models of [25] have been used to succesfully reveal the occurrence of AGB dominated GCs in the merger remnant galaxy NGC 7252 ([27]; Figure 5).

It is also shown that SSP models using uncalibrated stellar tracks for the TP-AGB fail to reproduce the Magellanic Clouds GCs colours. As mentioned in Section 3.4, the TP-AGB phase is included semi-empirically also by [11], and the AGB bolometric contribution is calibrated with Magellanic Clouds GCs, like in Figure 4. However, the SSP integrated colours (dashed line in Figure 3) do not exhibit the required "jump" in V−K displayed by these GCs. This might be due to the fact that in their models the contribution by the sole TP-AGB never exceeds $\sim$ 10% (Figure 10 in [11]), at variance with Figure 4.

The influence of nebular continua. The SED of very young stellar populations located in starforming regions may be affected by emission from gas. This is what the models of the Starburst99 group ([23]) try to account for. Specifically designed for active starforming regions, these models include also emission

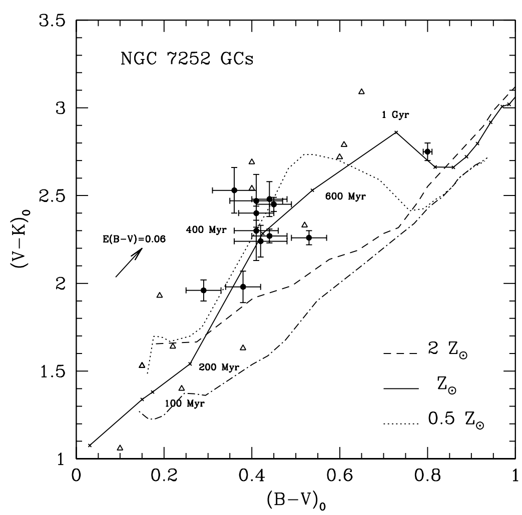

Fig. 5. Detection of AGB-dominated GCs in an external galaxy. Same diagram as in Figure 4 for the GCs of the merger remnant galaxy NGC 7252 (filled symbols). From [27].

lines from interstellar components. The TP-AGB phase is not included in these models, that are therefore appropriate for ages smaller than ~ 100 Myr.

High-resolution SSPs [46] presents high spectral resolution (1.8 Å) SEDs of old SSPs. These are obtained by using empirical stellar libraries instead of the Kurucz model atmospheres. The advantage is that the observed spectra can be directly compared with the models without degrading their resolution. However, the presently very limited empirical libraries permit to model only a rather narrow range in ages and metallcities.

Model Lick indices for non solar chemistries The ratio of α-elements to Fe-peak elements ($[\alpha/\mathrm{Fe}]$) is a key diagnostic for the formation timescales of the stellar populations in galaxies (e.g. [40]). However, the standard model Lick indices (Section 3.5) are inadequate to study stellar populations with $[\alpha/\mathrm{Fe}] \neq 0$. This is demonstrated by the calibration of these type of models up to $Z_\odot$ ([28]), accomplished with the metal-rich ($Z \sim Z_\odot$) and $[\alpha/\mathrm{Fe}] = 0.3$ GCs NGC 6528 and NGC 6553 of the galactic Bulge (Figure 6, [28]). The model comparison with galactic GCs with lower metallicities shows that the standard models reflect non solar $[\alpha/\mathrm{Fe}]$ at subsolar metallicities. This *variable* $[\alpha/\mathrm{Fe}]$ of the standard models results from the calibrating stars used to compute the fitting functions ([28]). To derive the abundances of unresolved extra-galactic stellar populations it is desirable to have models with well-defined values of element abundance ratios. [39]

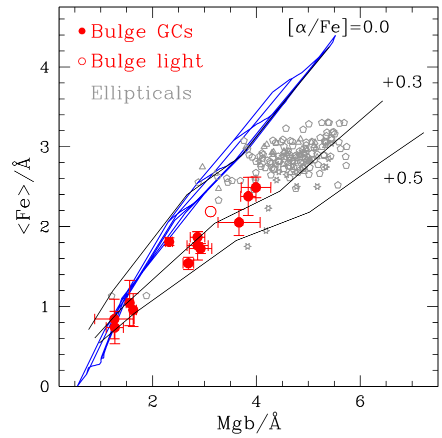

Fig. 6. From [28]. Calibration of standard model Lick indices (grid) with GCs including Bulge objects (filled large symbols, from [30]) The three thick lines show the models by [39] with a constant age of 12 Gyr and three values of the [α/Fe] ratios. The large empty circle is the average Bulge field in Baade window. Small symbols are data of ellipticals from various samples.

provide such *new generation* models, that for the first time are given as functions of element abundances (e.g. the [α/Fe] ratio) and for various values of [α/Fe], [α/Ca], [α/N], etc. To establish their adequacy, these models for [α/Fe]=0.3 are calibrated with GCs (thick lines in Figure 6).

Horizontal Branch morphology and age confusion The morphology of the HB impacts on Balmer lines and broad band colours. We focus here on Balmer lines, since they are widely used as age indicators for GCs. The degeneracy age-HB morphology arises from the fact that the blue HBs of metal-poor GCs enhance their integrated Hβ values, that become larger than those of coeval GCs with red HBs. The bluer HBs at decreasing metallicity are due to, as a first parameter, hotter stars at lower metallicity. As a second parameter to the mass-loss along the RGB, which by removing stellar envelope, shifts the $T_{\rm eff}$ of the stars to higher values. Therefore the Balmer lines of coeval stellar populations *increase* with decreasing metallicity, which undermines their power as age indicators ([26]). As mentioned in Section 2.2, the assumed mass loss in SSP models must be calibrated a posteriori. [26] calibrate the mass-loss required to reproduce the Hβ line observed in galactic GCs as a function of metallicity. An updated version of that calibration, which extends to higher-order Balmer lines with the aid of new data is shown in Figure 7 (from [28]). The age ambiguity induced by the HB morphology is nicely illustrated by the four GCs at [Z/H] ~ -0.6. Two of them (NGC 6441 and NGC 6338) have blue HB stars, which are responsible for their rather large Hβ's ($\sim$ 2 Å). Note that if this effect is not accounted for, these two GCs would appear considerably younger ($\sim$ 8 Gyr) than those

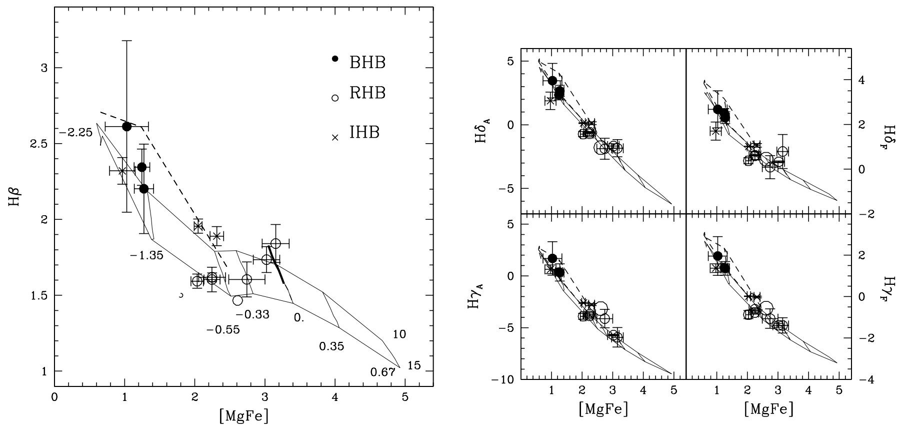

Fig. 7. Calibration of Balmer lines vs. HB morphology with galactic GCs, from [28]. Left-hand panel: Hβ; right-hand panel: Hδ_A, Hγ_A, Hδ_F and Hγ_F. HB morphologies of GCs are coded, in which RHB, BHB and IHB refer to red, blue and intermediate HBs, respectively. Dashed line: 15 Gyr old SSPs with various [Z/H] (labelled) and canonical mass-loss. Solid lines: 15 and 10 Gyr old models (for same [Z/H]) in which no mass loss has been assumed, in order to mimic reddish HB morphologies.

with same [Z/H] that lie on the 15 Gyr old SSP, in spite of the very similar ages derived from their MS turnoff.

References

1. N. Arimoto, Y. Yoshii: A&A **164**, 260 (1986)
2. G. Barbaro, B.M. Poggianti: A&A **324**, 490 (1997)
3. M.S. Bessel, J.M. Brett, M. Scholz, P.R. Wood: A&A **213**, 209 (1989)
4. A.C. Borges, T.P. Idiart, J.A. de Freitas Pacheco, F. Thevenin: AJ **110**, 2408 (1995)
5. G. Bruzual: ApJ **273**, 105 (1983)
6. G. Bruzual & S. Charlot: ApJ **405**, 538 (1993)
7. A. Buzzoni: ApJS **71**, 827 (1989)
8. A. Buzzoni, G. Gariboldi, L. Mantegazza: AJ **103**, 1814 (1992)
9. A. Buzzoni, G. Gariboldi, L. Mantegazza: AJ **107**, 513 (1994)
10. S. Cassisi, V. Castellani, S. degl'Innocenti, M. Salaris, A. Weiss: A&AS **134**, 103 (1999)
11. S. Charlot, G. Bruzual: ApJ **367**, 126 (1991)
12. S. Charlot, G. Worthey, A. Bressan: ApJ **457**, 625 (1996)
13. C. Chiosi, G. Bertelli, A. Bressan: A&A **196**, 84 (1988)
14. J.F. Crampin, F. Hoyle: MNRAS **122**, 28 (1961)
15. F. Fagotto, A. Bressan, G. Bertelli, C. Chiosi: A&AS **105**, 29 (1994)
16. S.M. Faber: A&A **20**, 361 (1972)
17. L. Girardi, G. Bertelli: MNRAS **300**, 533 (1998)
18. J.E. Gunn, L.L. Stryker, B. M. Tinsley: ApJ **249**, 48 (1981)

19. T. Kodama, N. Arimoto: A&A **320**, 41 (1997)
20. R.L. Kurucz: ApJS **40**, 1 (1979)
21. H.L. Johnson: ARA&A **4**, 193 (1966)
22. Th. Lejeune, F. Cuisinier, R. Buser: A&AS **125**, 229, (1997)
23. C. Leitherer et al.: ApJS **123**, 3 (1999)
24. A. Maeder, G. Meynet: A&A **210**, 155 (1989)
25. C. Maraston: MNRAS **300**, 872 (1998)
26. C. Maraston, D. Thomas: ApJ **541**, 126 (2000)
27. C. Maraston, M. Kissler-Patig, J.P. Brodie, P. Barmby, J. Huchra: A&A **370**, 176 (2001)
28. C. Maraston, L. Greggio, A. Renzini, et al: A&A *in press*, astro-ph/0209220, (2002)
29. G. Piotto, et al.: A&A **391**, 945 (2002)
30. T.H. Puzia, M. Kissler-Patig, R.P. Saglia, C. Maraston, et al.: A&A **395**, 45 (2002)
31. A. Renzini: AnnPhysFR **6**, 87 (1981)
32. A. Renzini, A. Buzzoni: "Global properties of stellar populations and the spectral evolution of galaxies". In *Spectral evolution of galaxies*, Proceedings of the Fourth Workshop, Erice, Italy, March 12-22, 1985, ed. by C. Chiosi, A. Renzini (Dordrecht: Reidel 1986), pp. 195-231
33. A. Renzini: "Spectral evolution of galaxies - A theoretical viepoint". In *Stellar populations*, Baltimore, MD, May 20-22, 1986, ed. by C. Chiosi, A. Renzini, J. Dyson, (Cambridge University Press, 1986) pp. 213-223
34. A. Renzini: in *Galaxy Formation*, eds. J. Silk, N. Vittorio, (Amsterdam: Holland, 1994), p. 303
35. A. Renzini, F. Fusi Pecci: ARA&A **6**, 199 (1988)
36. B. Rocca-Volmerange & B. Guiderdoni: A&A **175**, 15 (1987)
37. B. Salasnich, B., L. Girardi, A. Weiss, C. Chiosi: A&A **361**, 1023 (2000)
38. R. Tantalo et al.: A&A **311**, 361 (1996)
39. D. Thomas, C. Maraston, R. Bender: MNRAS *in press* astro-ph 0209250 (2002)
40. D. Thomas, L. Greggio, R. Bender: MNRAS **302**, 537 (1999)
41. B.M. Tinsley: ApJ **151**, 547 (1968)
42. B.M. Tinsley: A&A **20**, 383 (1972)
43. B.M. Tinsley: ApJ **186**, 35 (1973)
44. B.M. Tinsley, J.E Gunn: ApJ **203**, 52 (1976)
45. D.A. VandenBerg et al.: ApJ **532**, 430 (2000)
46. A. Vazdekis: ApJ **513**, 224 (1999)
47. A. Vazdekis et al.: ApJS **111**, 203 (1996)
48. P. Westera et al.: A&A **381**, 524 (2002)
49. G. Worthey: ApJS **95**, 107 (1994)
50. G. Worthey, S.M. Faber, J.J. González, D. Burstein: ApJS **94**, 687 (1994)